Atomic Data and Nuclear Data Tables 140 (2021) 101440

Contents lists available at ScienceDirect

Atomic Data and Nuclear Data Tables

journal homepage: www.elsevier.com/locate/adt

Compilation of recent nuclear ground state charge radius measurements and tests for models

Tao Li [a,b,*], Yani Luo [a], Ning Wang [a,b,**]

[a] Department of Physics, Guangxi Normal University, Guilin, 541004, PR China
[b] Guangxi Key Laboratory of Nuclear Physics and Technology, Guilin, 541004, PR China

ARTICLE INFO

Article history:
Received 21 January 2021
Received in revised form 17 April 2021
Accepted 19 April 2021
Available online 7 May 2021

Keywords:
Nuclear charge radius
Shell effect
Mirror nuclei
Isospin asymmetry

ABSTRACT

The root-mean-square (rms) charge radii of 236 nuclides measured by laser spectroscopy experiment are compiled, and the uncertainties are calculated. From the rms charge radii of Mg isotope chain, the new magic number $N = 14$ can be observed, and the traditional magic number $N = 20$ disappears in the K isotope chain. A good linear relationship between the difference of the mirror nuclear charge radii and the isospin asymmetry can be clearly observed with a Pearson's linear correlation coefficient of 0.96. The accuracies and predictive powers of the WS* and HFB25 models are tested with these new data. The rms deviation with the WS* model is only 0.0176 fm for the 129 new data, which is much better than that of HFB25 model. The influence of deformation effect on nuclear charge radius prediction is studied systematically.

* Corresponding author at: Department of Physics, Guangxi Normal University, Guilin, 541004, PR China.
** Corresponding author.
E-mail addresses: litao@gxnu.edu.cn (T. Li), wangning@gxnu.edu.cn (N. Wang).

https://doi.org/10.1016/j.adt.2021.101440
0092-640X/

Contents

1. Introduction

As one of the static properties in atomic nuclei, nuclear charge radius is a key observable that can directly reflect the important characteristics on the nuclear structure. For instance, nuclear charge radius could give signals for the occurrence of new magic number or the disappearance of traditional magic number considering the influence of shell effect on charge radii [1–3]. In addition, it is useful for the study of neutron skin, neutron halo and isomer [4–6]. So far, the root-mean-square (rms) charge radii of more than 1000 nuclei have been measured by two types of experiments in general: (i) the charge radii of stable nuclei were measured by charged particle scattering experiment, (ii) the charge radii of radionuclides were measured by charge radii changes $\delta\langle r^2\rangle$ extracted from laser spectroscopy and K_α *X-ray* isotope shifts [7,8]. In recent years, with the development of experiment technology, more and more rms charge radii of unstable nuclei have been measured for the first time by charge radii changes $\delta\langle r^2\rangle$[9–35] from laser spectroscopy experiments. It is therefore interesting to systematically study the new experimental data.

In the beginning, the nuclear charge radius R_o is usually described by the $A^{1/3}$ law: $R_o = r_0 A^{1/3}$, where A is the mass number. With more experimental data being obtained, it was found that the isospin and shell effects also play very important roles for the charge radius [2,36–41]. The rms nuclear charge radius can be self-consistently calculated by using microscopic nuclear mass models, such as the Skyrme–Hartree–Fock–Bogoliubov (HFB) model [42,43] and the relativistic mean field (RMF) model [44,45]. In addition, the nuclear charge radius can also be predicted by using some local relations [46–48] such as the Garvey–Kelson relations (GKRs). It is necessary to test the predictive power of these different models for the description of nuclear charge radius based on new measured data. In addition, nuclear rms charge radius is closely related to deformation parameters. It is therefore interesting to study the influence of deformation parameters on the calculation of nuclear rms charge radius.

The structure of this paper is as follows: In Section 2, 236 experimental data for nuclear rms charge radii from laser spectroscopy experiments are compiled and the corresponding uncertainties are analyzed. The influence of shell effect on the charge radius will be also investigated for Mg and K isotope chains in this section. In Section 3, the accuracy and predictive power of the two models will be tested based on these new experimental data, and the influence of different deformation parameters on the calculation of nuclear rms charge radii will be analyzed. Finally, a summary will be given in Section 4.

2. New data on nuclear charge radii

The mean square charge radius difference $\delta\langle r^2\rangle^{A'A} = \langle r^2\rangle^A - \langle r^2\rangle^{A'}$ between isotopes can be obtained from the isotope shift based on laser spectroscopy experiment. Therefore, mean square charge radius can be written as $\langle r^2\rangle^A = \langle r^2\rangle^{A'} + \delta\langle r^2\rangle^{A'A}$. The rms charge radius can be calculated from the following formula

$$r_c(A) = \sqrt{\langle r^2\rangle^A} = \sqrt{\langle r^2\rangle^{A'} + \delta\langle r^2\rangle^{A'A}} \tag{1}$$

where A' represents the mass number of stable reference isotope. According to the calculation method of uncertainty, the uncertainty of nuclear rms charge radius from experiment can be expressed as

$$\triangle r_c(A) = r_c(A) \cdot \frac{\sqrt{4r_c^2(A')\cdot(\triangle r_c(A'))^2 + (\triangle\delta\langle r^2\rangle^{A'A})^2}}{2[r_c^2(A') + \delta\langle r^2\rangle^{A'A}]} \tag{2}$$

where $r_c(A')$ and $\triangle r_c(A')$ are the rms charge radius and uncertainty of A' isotope, $\triangle\delta\langle r^2\rangle^{A'A}$ is the uncertainty of the mean square charge radius difference $\delta\langle r^2\rangle^{A'A}$ and extracted from experimental statistical and systematic errors. Usually, the literature will present the corresponding statistical and systematic errors as well as the mean square charge radius difference of isotopes. Using Eqs. (1) and (2), we obtain 236 experimental data of nuclear charge radius measured by laser spectroscopy experiment and calculate the corresponding uncertainties, which are listed in Table 1, where $r_c(A')$ is taken from Ref. [1] and has been set in bold in Table 1. Compared with the data in Ref. [1], there are 130 new experimental data. It is worth noting that the rms charge radii of 106 nuclei in Table 1 are slightly different from the published results in Ref. [1], which may be caused by the fact that the original experimental data were selected from different experimental groups or different experimental measurement methods were adopted. We checked the uncertainties calculated by Eq. (2) and found that our results for Be isotope are in agreement with the results in Ref. [9]. Fig. 1 shows the uncertainties of rms charge radius for $Z = 29$ and 48 isotope chains calculated by Eq. (2). One can see from Fig. 1, the uncertainties obviously increase with the distance from isotope A' (dotted line position). The uncertainties of rms charge radius of other isotopic chains measured by laser spectroscopy have similar characteristics.

The nuclear shell effect is one of the important microscopic quantum effects in nuclear physics. We will focus on the effect of neutron shell on charge radius in isotope chains. Similar to neutron shell gap of nuclear mass, we define the neutron gap of charge radius as follows:

$$\Delta_n^{r_c}(N,Z) = r_c(N-2,Z) + r_c(N+2,Z) - 2r_c(N,Z) \tag{3}$$

where $r_c(N,Z)$ is the measured nuclear rms charge radii. In Fig. 2, we show the trend of neutron gaps of charge radii of Mg and K isotope chains. For K isotope chain, one can clearly see the peak at the magic number $N = 28$. However, the enhancement of $\Delta_n^{r_c}$ cannot be observed at the magic number $N = 20$. A similar behavior can also be observed in the Ar and Ca isotope chains. It is known that the doubly magic nuclei are spherical in shape, the abrupt change trend of the charge radius at the magic number could be due to the shell effect in nucleus. For Mg isotope chain, the peak at $N = 14$ can be clearly observed in the trend of

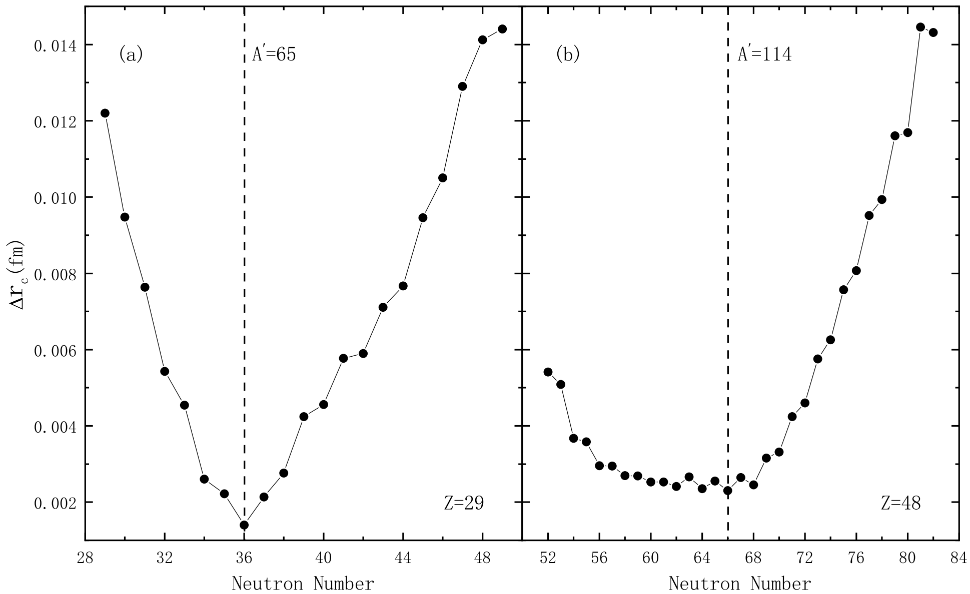

Fig. 1. Uncertainties of rms charge radii for $Z = 29$ and $Z = 48$ isotope chains are calculated by Eq. (2).

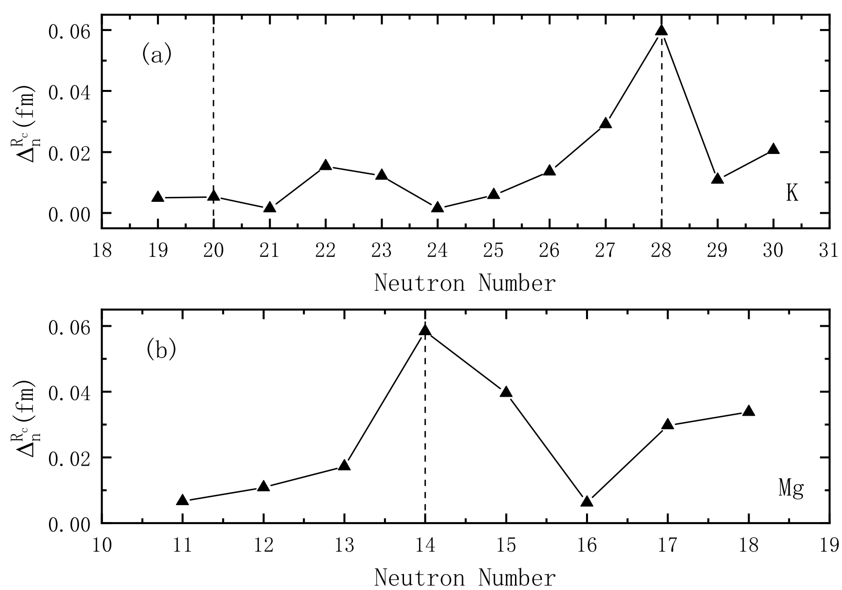

Fig. 2. Neutron gaps of charge radii of K and Mg isotope chains as a function of neutron number.

neutron gaps of charge radii, which implies that $N = 14$ could be a new magic number. In addition, the evidence that $N = 14$ is a magic number can also be seen from the trend of the two-neutron separation energy with the neutron number. Recently, S. Bagchi et al. also found the evidence for magic number $N = 14$ from the proton radii of N isotope chain [49].

In the absence of coulomb interactions between protons, a perfectly charge-symmetric and charge-independent nuclear force would result in the binding energies of mirror nuclei (i.e. nuclei with the same atomic number A but with the proton number Z and neutron number N interchanged) being identical. The neutron skin thickness of a neutron-rich nucleus should be very close to the proton skin thickness of its mirror nucleus, if we remove the coulomb interactions. Considering the difficulties in the measurement of neutron skin thickness, it is interesting to study the difference of charge radii between mirror nuclei. We study the relationship between the difference in mirror nuclei charge radii and the isospin asymmetry $I = (N - Z)/A$. A good linear relationship between them can be observed from Fig. 3, and Pearson's linear correlation coefficient $P = 0.96$. It indicates that the difference of mirror nuclear charge radii could be useful for the study of symmetry energy at saturated densities [2].

3. Tests of the theoretical methods for nuclear charge radii

In Ref. [2], considering the isospin and shell effects in the nucleus, a four-parameter nuclear charge radii formula was proposed by combining the shell corrections and deformations of nuclei obtained from the Weizsäcker–Skyrme (WS*) mass model [50]. The expression is shown below

$$r_c = \sqrt{\frac{3}{5}}[1.226A^{1/3} + 2.86A^{-2/3} - 1.09I(1-I) + 0.99\Delta E/A] \times [1 + \frac{5}{8\pi}(\beta_2^2 + \beta_4^2)] \quad (4)$$

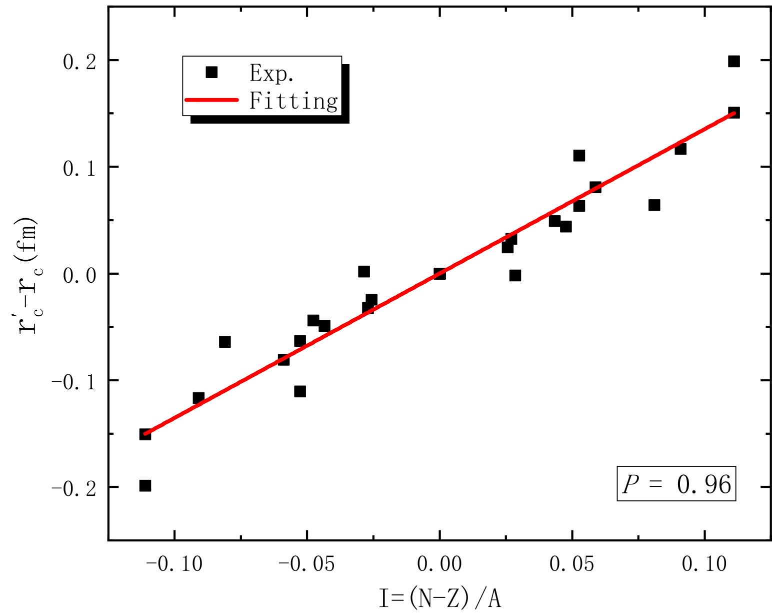

Fig. 3. (Color online) Linear relationship between the difference of mirror nuclei charge radii and isospin asymmetry I, where r_c and r_c' represent the rms charge radii of nuclei and its corresponding mirror nuclei, respectively.

where A is the mass number, I is the isospin asymmetry, ΔE denotes the shell corrections, β_2 and β_4 represent the quadrupole and hexadecimal deformation of the nucleus, respectively. The 885 measured rms charge radii of the nuclei from Ref. [1] were reproduced by this formula with an rms deviation $\sigma = \sqrt{\frac{1}{n}\sum_{i=1}^{n}(r_c^{exp} - r_c^{th})^2} = 0.022$ fm. In addition, Hartree–Fock–Bogoliubov (HFB) mass models [42,43] were successfully proposed for describing nuclear properties, such as nuclear mass and charge radius. The corresponding rms deviation with respect to the 884 measured charge radii is 0.025 fm from the HFB25 model calculations [42], which is comparable to the results of WS* model (Eq. (4)). It is interesting to test the predictive power of these two models based on the latest experimental data of nuclear charge radius.

Fig. 4(a) shows the deviation between the measured rms charge radii for 1014 nuclei and model predictions. The rms deviations are 0.0213 fm from WS* model and 0.0254 fm from the HFB25 model, respectively. In Table 1, we list the predictions of these two models for 129 new measured charge radii. Fig. 4(b) shows the difference between the experimental data and model predictions for the 129 new charge radii. One can see results of the WS* model are much better than those of HFB25 model.

In addition to the difference in describing the ground state mass of nucleus, it is also different for the HFB25 and WS* models in describing the ground state charge radius of nucleus. Literature [51] also shows that the deformation energies of the HFB25 model are systematically larger than those of the WS* model, especially for light and intermediate nuclei. Since it is difficult to directly measure the nuclear deformation parameters experimentally, it is necessary to study the influence of deformation parameters on the prediction of nuclear charge radius. We introduce a correction coefficient r_β of the deformation parameter in Eq. (4), and the expression is as follows.

$$r_c = \sqrt{\frac{3}{5}}[r_0A^{1/3} + r_1A^{-2/3} + r_sI(1-I) + r_d\Delta E/A][1 + \frac{5r_\beta}{8\pi}(\beta_2^2 + \beta_4^2)] \tag{5}$$

The introduction of the coefficient r_β may further improve the predictions of the rms charge radius due to the inaccuracy of the deformation parameters given by the theoretical model. Of course, it also checks the overall behavior of the deformation parameters given by the theoretical model, because if the deformation parameters are extremely accurate, the coefficient r_β should be strictly equal to 1.

The coefficients in Eq. (5) can be obtained by fitting the latest 1014 experimental data of atomic nuclei rms charge radii based on the shell correction energies and deformation parameters provided by different nuclear mass models, which are listed in Table A. The data in the first and second rows in Table A are obtained by fitting the latest experimental data when the deformation correction coefficient $r_\beta = 1$, which is actually equivalent to the new parameters in Eq. (4). First of all, it can be seen from the third column of Table A that although a deformation correction coefficient is added to the formula, the rms deviation is only reduced by 2.3% with the shell correction energies and deformation parameters provided by the WS* mass model. However, the rms deviation obtained by fitting the experimental data with deformation parameters provided by the HFB25 mass model is reduced by 11.2%. It indicates that deformation parameters significantly influence the calculation of nuclear charge radius. It is worth mentioning that the optimally obtained coefficients in Eq. (5) and rms deviation based on the deformation parameters and shell corrections from the latest WS4 mass model [52] are very close to those from the WS* mass model. From the value of r_β in Table A, it seems that the deformation parameters given by the WS* mass model are underpredicted, while the deformation parameters given by the HFB25 mass model are overpredicted. For the prediction of charge radii of deformed nuclei, the formula in Eq. (5) could give better results.

4. Summary

In this work, we compiled the rms charge radii of 236 nuclides measured by laser experiment, and systematically calculated the uncertainties. The new magic number $N = 14$ was observed in the Mg isotope chain based on the neutron gaps of charge radii, and the traditional magic number $N = 20$ disappeared in the K isotope chain. A good linear relationship between the difference of the mirror nuclear charge radii and the isospin asymmetry

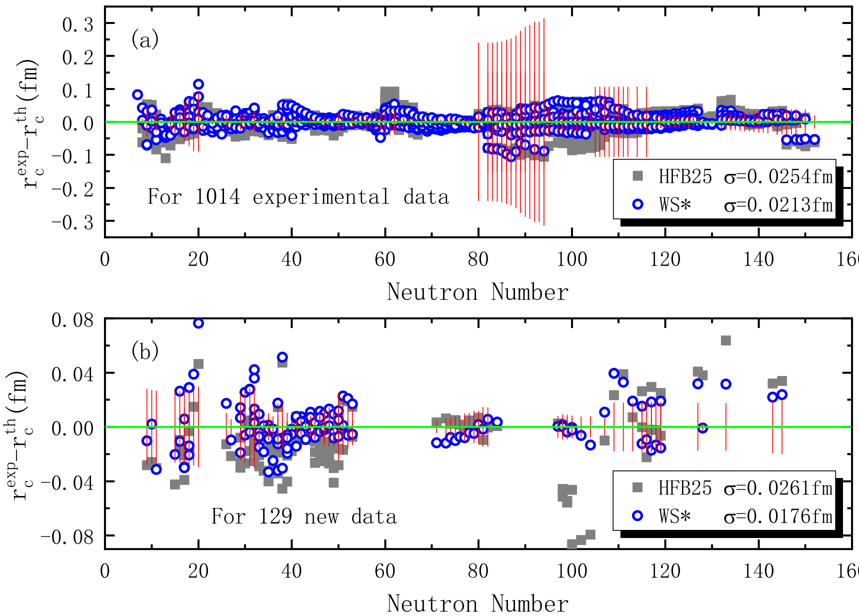

Fig. 4. Difference between the experimental data and model calculations for the rms nuclear charge radius. The circles and squares denote the results of the WS* and HFB25 models, respectively. The red error bars denote the uncertainty of the experimental data. (For interpretation of the references to color in this figure legend, the reader is referred to the web version of this article.)

Table A
Parameters in Eq. (5) obtained by fitting latest experimental data, the shell correction energies from the WS* mass model and the deformation parameters from the WS* and HFB25 mass models. The first column indicates which model the deformation parameters are taken from. The second column represents the number of experimental data required for fitting. The third column represents the rms deviation.

Model	N_{nucl}	σ (fm)	r_0	r_1	r_s	r_d	r_β
WS*	1014	0.0214	1.225	2.884	−1.066	0.948	1
HFB25	1013	0.0286	1.217	3.023	−0.972	0.647	1
WS*	1014	0.0209	1.224	2.916	−1.086	0.920	1.213
HFB25	1013	0.0254	1.222	2.903	−0.963	0.830	0.600

was clearly observed with a Pearson's linear correction coefficient of 0.96. We tested the accuracies and predictive powers of the WS* and HFB25 models based on the new experimental data of charge radius. The rms deviation between predictions from the WS* model and 1014 known charge radii is 0.0213 fm, and the rms deviation between predictions from the HFB25 model and 1013 known charge radii is 0.0254 fm. The rms deviation between the predicted results of the WS* model and the 129 new experimental value is only 0.0176 fm, smaller by 20% than the results with respect to the 885 experimental data. The corresponding result for the HFB25 model is 0.0261 fm, which is larger by 4.4% than the previous results of the 884 experimental data. In addition, we find that deformation parameters have an obvious influence on the prediction of nuclear charge radius. For a better consideration of the influence of deformation parameters on the prediction of nuclear charge radius, the charge radii formula is revised. The deformation parameters from the WS* and HFB25 mass models are roughly evaluated by using Eq. (5) and newest 1014 experimental data of nuclear rms charge radii. We find that the deformation parameters given by the WS* mass model are slightly underpredicted, while those given by HFB25 mass model are overpredicted.

Declaration of competing interest

The authors declare that they have no known competing financial interests or personal relationships that could have appeared to influence the work reported in this paper.

Acknowledgments

This work was supported by the National Natural Science Foundation of China (Grant No. U1867212, 12047567), the Natural Science Foundation of Guangxi (Grant No. 2017GXNSFGA198001) and the Middle-aged and Young Teachers' Basic Ability Promotion Project of Guangxi (CN) (Grant No. 2019KY0061).

References

[1] I. Angeli, K.P. Marinova, At. Data Nucl. Data Tables 99 (2013) 69.
[2] N. Wang, T. Li, Phys. Rev. C 88 (2013) 011301, (R).
[3] I. Angeli, K.P. Marinova, J. Phys. G: Nucl. Part. Phys. 42 (2015) 055108, 20pp.
[4] W. Geithner, T. Neff, G. Audi, et al., Phys. Rev. Lett. 101 (2008) 252502.
[5] W. Nörtershäuser, D. Tiedemann, M. Žáková, et al., Phys. Rev. Lett. 102 (2009) 062503.
[6] D.T. Yordanov, D.L. Balabanski, M.L. Bissell, et al., Phys. Rev. Lett. 116 (2016) 032501.
[7] K. Marinova, J. Phys. Chem. Ref. Data 44 (3) (2015) 031214.
[8] I. Angeli, K. Marinova, J. Phys. Conf. Ser. 724 (2016) 012032.
[9] A. Krieger, K. Blaum, M.L. Bissell, et al., Phys. Rev. Lett. 108 (2012) 142501.
[10] D.T. Yordanov, M.L. Bissell, K. Blaum, et al., Phys. Rev. Lett. 108 (2012) 042504.
[11] D.M. Rossi, K. Minamisono, H.B. Asberry, et al., Phys. Rev. C 92 (2015) 014305.
[12] A.J. Miller, K. Minamisono, A. Klose, et al., Nat. Phys. 15 (2019) 432.
[13] R.F. Garcia Ruiz, M.L. Bissell, K. Blaum, et al., Nat. Phys. 12 (2016) 594.
[14] H. Heylen, C. Babcock, R. Beerwerth, et al., Phys. Rev. C 94 (2016) 054321.
[15] K. Minamisono, D.M. Rossi, R. Beerwerth, et al., Phys. Rev. Lett. 117 (2016) 252501.
[16] S. Kaufmann, J. Simonis, S. Bacca, et al., Phys. Rev. Lett. 124 (2020) 132502.
[17] M.L. Bissell, T. Carette, K.T. Flanagan, et al., Phys. Rev. C 93 (2016) 064318.
[18] R.P. de Groote, J. Billowes, C.L. Binnersley, et al., Nat. Phys. 16 (2020) 620.
[19] L. Xie, X.F. Yang, C. Wraith, et al., Phys. Lett. B 797 (2019) 134805.
[20] T.J. Procter, J. Billowes, M.L. Bissell, et al., Phys. Rev. C 86 (2012) 034329.
[21] G.J. Farooq-Smith, A.R. Vernon, J. Billowes, et al., Phys. Rev. C 96 (2017) 044324.
[22] E. Mané, A. Voss, J.A. Behr, et al., Phys. Rev. Lett. 107 (2011) 212502.
[23] T.J. Procter, J.A. Behr, J. Billowes, et al., Eur. Phys. J. A 51 (2015) 23.
[24] R. Ferrer, N. Bree, T.E. Cocolios, et al., Phys. Lett. B 728 (2014) 191.
[25] M. Hammen, W. Nörtershäuser, D.L. Balabanski, et al., Phys. Rev. Lett. 121 (2018) 102501.
[26] C. Gorges, L.V. Rodríguez, D.L. Balabanski, et al., Phys. Rev. Lett. 122 (2019) 192502.

[27] K.T. Flanagan, J. Billowes, P. Campbell, et al., J. Phys. G: Nucl. Part. Phys. 39 (2012) 125101.
[28] B.A. Marsh, T. Day Goodacre, S. Sels, et al., Nat. Phys. 14 (2018) 1163.
[29] A.E. Barzakh, A.N. Andreyev, T.E. Cocolios, et al., Phys. Rev. C 95 (2017) 014324.
[30] A.E. Barzakh, L. Kh. Batist, D.V. Fedorov, et al., Phys. Rev. C 88 (2013) 024315.
[31] A.E. Barzakh, D.V. Fedorov, V.S. Ivanov, et al., Phys. Rev. C 97 (2018) 014322.
[32] M.D. Seliverstov, T.E. Cocolios, W. Dexters, et al., Phys. Lett. B 719 (2013) 362.
[33] D.A. Fink, T.E. Cocolios, A.N. Andreyev, et al., Phys. Rev. X 5 (2015) 011018.
[34] K.M. Lynch, J. Billowes, M.L. Bissell, et al., Phys. Rev. X 4 (2014) 011055.
[35] K.M. Lynch, S.G. Wilkins, J. Billowes, et al., Phys. Rev. C 97 (2018) 024309.
[36] Bożena Nerlo-Pomorska, Z. Krzysztof Pomorski, Phys. A 344 (1993) 359.
[37] Bożena Nerlo-Pomorska, Z. Krzysztof Pomorski, Phys. A 348 (1994) 169.
[38] I. Angeli, N.S. Aph, Heavy Ion Phys. 13 (2001) 149.
[39] I. Angeli, At. Data Nucl. Data Tables 87 (2004) 185.
[40] R.H. Li, Y.M. Hu, M.C. Li, Physica C 33 (2009) 123, (Suppl. I).
[41] Z.Q. Sheng, G.W. Fan, J.F. Qian, et al., Eur. Phys. J. A 51 (2015) 40.
[42] S. Goriely, N. Chamel, J.M. Pearson, Phys. Rev. C 88 (2013) 024308.
[43] S. Goriely, N. Chamel, J.M. Pearson, Phys. Rev. C 88 (2013) 061302, (R).
[44] G.A. Lalazissis, S. Raman, P. Ring, At. Data Nucl. Data Tables 71 (1999) 1.
[45] P.W. Zhao, Z.P. Li, J.M. Yao, et al., Phys. Rev. C 82 (2010) 054319.
[46] J. Piekarewicz, M. Centelles, X. Roca-Maza, et al., Eur. Phys. J. A 46 (2010) 379.
[47] B.H. Sun, Y. Lu, J.P. Peng, et al., Phys. Rev. C 90 (2014) 054318.
[48] M. Bao, Y. Lu, Y.M. Zhao, et al., Phys. Rev. C 94 (2016) 064315.
[49] S. Bagchi, R. Kanungo, W. Horiuchi, et al., Phys. Lett. B 790 (2019) 251.
[50] N. Wang, Z.Y. Liang, M. Liu, et al., Phys. Rev. C 82 (2010) 044304.
[51] N. Wang, T. Li, Acta Phys. B. Pro. Sup. 12 (2019) 715.
[52] N. Wang, M. Liu, X.Z. Wu, et al., Phys. Lett. B 734 (2014) 215.

Explanation of Tables

Table 1. The experimental data of rms charge radii for 236 nuclei

Z	The atomic (proton) number.
el.	The element symbol.
N	The neutron number.
A	The mass number.
$\delta\langle r^2\rangle$	The mean square charge radius difference comes from the corresponding references, as shown below.
$\Delta\delta\langle r^2\rangle$	The error of the mean square charge radius difference $\Delta\delta\langle r^2\rangle = \sqrt{\triangle^2_{sta.} + \triangle^2_{sys.}}$, where $\triangle_{sta.}$ and $\triangle_{sys.}$ represent the statistical error and systematic error of $\delta\langle r^2\rangle$ respectively, from the corresponding references.
r_c	The experimental data of nuclear rms charge radius, it is calculated by Eq. (1).
Δr_c	The uncertainty of nuclear rms charge radius, it is calculated by Eq. (2).
In Ref. [1]	Specifies if the nuclear charge radius measurement was included in Ref. [1]

(1) The mean square charge radius differences $\delta\langle r^2\rangle$ of $^{7,9-12}$Be from Ref. [9].
(2) The mean square charge radius differences $\delta\langle r^2\rangle$ of $^{21-32}$Mg from Ref. [10].
(3) The mean square charge radius differences $\delta\langle r^2\rangle$ of $^{36-51}$K from Ref. [11].
(4) The mean square charge radius differences $\delta\langle r^2\rangle$ of $^{36-39}$Ca and $^{43-52}$Ca from Refs. [12] and [13] , respectively.
(5) The mean square charge radius differences $\delta\langle r^2\rangle$ of $^{50-64}$Mn from Ref. [14].
(6) The mean square charge radius differences $\delta\langle r^2\rangle$ of ^{52,53}Fe from Ref. [15].
(7) The mean square charge radius differences $\delta\langle r^2\rangle$ of ^{58,61,62,64,68}Ni from Ref. [16].
(8) The mean square charge radius differences $\delta\langle r^2\rangle$ of $^{58-75}$Cu and $^{76-78}$Cu from Refs. [17] and [18] , respectively.
(9) The mean square charge radius differences $\delta\langle r^2\rangle$ of $^{62-80}$Zn from Ref. [19].
(10) The mean square charge radius differences $\delta\langle r^2\rangle$ of $^{63-82}$Ga from Refs. [20,21].
(11) The mean square charge radius differences $\delta\langle r^2\rangle$ of $^{74-76}$Rb from Refs. [22,23].
(12) The mean square charge radius differences $\delta\langle r^2\rangle$ of $^{97-101,107}$Ag from Ref. [24].
(13) The mean square charge radius differences $\delta\langle r^2\rangle$ of $^{100-130}$Cd from Ref. [25].
(14) The mean square charge radius differences $\delta\langle r^2\rangle$ of even-A $^{108-134}$Sn from Ref. [26].
(15) The mean square charge radius differences $\delta\langle r^2\rangle$ of ^{175,177}Yb from Ref. [27].
(16) The mean square charge radius differences $\delta\langle r^2\rangle$ of $^{177-185}$Hg from Ref. [28].
(17) The mean square charge radius differences $\delta\langle r^2\rangle$ of $^{179-181,183}$Tl and $^{185,190-205,207,208}$Tl from Refs. [29] and [30], respectively.
(18) The mean square charge radius differences $\delta\langle r^2\rangle$ of ^{211,213}Bi from Ref. [31].
(19) The mean square charge radius differences $\delta\langle r^2\rangle$ of odd-A $^{193-203,209-211}$Po and ^{217,218}Po from Refs. [32] and [33], respectively.
(20) The mean square charge radius differences $\delta\langle r^2\rangle$ of $^{202-206}$Fr from Ref. [34].
(21) The mean square charge radius differences $\delta\langle r^2\rangle$ of $^{222-233}$Ra from Ref. [35].

Table 1
The experimental data of rms charge radii for 236 nuclei.

Z	el.	N	A	$\delta\langle r^2\rangle$ (fm^2)	$\Delta\delta\langle r^2\rangle$ (fm^2)	r_c (fm)	Δr_c (fm)	In Ref. [1]
4	Be	3	7	0.66	0.06	2.6468	0.0161	Yes
		5	**9**	**0**	–	**2.5190**	**0.0120**	Yes
		6	10	−0.77	0.05	2.3612	0.0166	Yes
		7	11	−0.26	0.04	2.4669	0.0147	Yes
		8	12	−0.08	0.05	2.5031	0.0157	No
12	Mg	9	21	0.176	0.068	3.0629	0.0114	No
		10	22	0.214	0.052	3.0691	0.0089	No
		11	23	0.053	0.035	3.0427	0.0063	No
		12	24	0.140	0.026	3.0570	0.0050	Yes
		13	25	−0.030	0.012	3.0291	0.0033	Yes
		14	26	0	–	3.0340	0.0026	Yes
		15	27	−0.008	0.011	3.0327	0.0031	No
		16	28	0.216	0.029	3.0694	0.0054	No
		17	29	0.256	0.037	3.0759	0.0065	No
		18	30	0.473	0.057	3.1110	0.0095	No
		19	31	0.710	0.081	3.1488	0.0131	No
		20	32	0.948	0.102	3.1864	0.0162	No
19	K	17	36	−0.16	0.10	3.4115	0.0148	No
		18	37	−0.08	0.07	3.4232	0.0104	No
		19	38	−0.089	0.025	3.4219	0.0041	Yes
		20	**39**	**0**	–	**3.4349**	**0.0019**	Yes
		21	40	0.016	0.023	3.4372	0.0038	Yes
		22	41	0.117	0.044	3.4519	0.0066	Yes
		23	42	0.111	0.065	3.4510	0.0096	Yes
		24	43	0.129	0.084	3.4536	0.0123	Yes
		25	44	0.122	0.102	3.4526	0.0149	Yes
		26	45	0.151	0.119	3.4568	0.0173	Yes
		27	46	0.092	0.136	3.4483	0.0198	Yes
		28	47	0.079	0.152	3.4464	0.0221	Yes
		29	48	0.264	0.168	3.4731	0.0243	No
		30	49	0.420	0.182	3.4955	0.0261	No
		31	50	0.513	0.197	3.5088	0.0281	No
		32	51	0.62	0.22	3.5240	0.0313	No
20	Ca	16	36	−0.196	0.027	3.4493	0.0044	No
		17	37	−0.205	0.023	3.4480	0.0038	No
		18	38	−0.0797	0.0064	3.4661	0.0021	No
		19	39	−0.1060	0.0064	3.4623	0.0021	Yes
		20	**40**	**0**	–	**3.4776**	**0.0019**	Yes
		23	43	0.114	0.009	3.4940	0.0023	Yes
		24	44	0.288	0.007	3.5188	0.0021	Yes
		25	45	0.125	0.009	3.4955	0.0023	Yes
		26	46	0.125	0.009	3.4955	0.0023	Yes
		27	47	0.002	0.010	3.4779	0.0024	Yes
		28	48	0.001	0.011	3.4777	0.0025	Yes
		29	49	0.098	0.013	3.4917	0.0027	No
		30	50	0.291	0.013	3.5192	0.0026	Yes
		31	51	0.392	0.014	3.5335	0.0027	No
		32	52	0.531	0.016	3.5531	0.0029	No
25	Mn	25	50	0.168	0.054	3.7283	0.0076	Yes
		26	51	0.065	0.067	3.7145	0.0093	Yes
		27	52	−0.226	0.034	3.6751	0.0051	Yes
		28	53	−0.285	0.022	3.6670	0.0037	Yes
		29	54	−0.166	0.013	3.6832	0.0028	Yes
		30	**55**	**0**	–	**3.7057**	**0.0022**	Yes
		31	56	0.053	0.016	3.7128	0.0031	Yes
		32	57	0.202	0.022	3.7329	0.0037	No
		33	58	0.234	0.030	3.7371	0.0046	No
		34	59	0.297	0.043	3.7456	0.0061	No
		35	60	0.329	0.048	3.7498	0.0068	No
		36	61	0.504	0.055	3.7731	0.0076	No
		37	62	0.615	0.064	3.7878	0.0087	No
		38	63	0.704	0.070	3.7995	0.0095	No
		39	64	0.873	0.078	3.8217	0.0104	No
26	Fe	26	52	0.282	0.075	3.7313	0.0102	No
		27	53	0.097	0.038	3.7064	0.0055	No
		28	**54**	**0**	–	**3.6933**	**0.0019**	Yes
28	Ni	30	58	−0.275	0.007	3.7756	0.0019	Yes
		32	**60**	**0**	–	**3.8118**	**0.0016**	Yes
		33	61	0.083	0.005	3.8227	0.0017	Yes
		34	62	0.223	0.005	3.8409	0.0017	Yes
		36	64	0.368	0.009	3.8598	0.0020	Yes

(continued on next page)

Table 1 (*continued*)

Z	el.	N	A	$\delta\langle r^2\rangle$ (fm^2)	$\Delta\delta\langle r^2\rangle$ (fm^2)	r_c (fm)	Δr_c (fm)	In Ref. [1]
		40	68	0.620	0.021	3.8923	0.0031	No
29	Cu	29	58	−0.833	0.092	3.7940	0.0122	No
		30	59	−0.635	0.072	3.8200	0.0095	No
		31	60	−0.511	0.058	3.8362	0.0077	No
		32	61	−0.359	0.041	3.8559	0.0055	No
		33	62	−0.293	0.034	3.8645	0.0046	No
		34	63	−0.148	0.017	3.8832	0.0026	Yes
		35	64	−0.116	0.014	3.8873	0.0023	No
		36	**65**	**0**	–	**3.9022**	**0.0014**	Yes
		37	66	0.033	0.013	3.9064	0.0022	No
		38	67	0.115	0.019	3.9169	0.0028	No
		39	68	0.133	0.032	3.9192	0.0043	No
		40	69	0.238	0.035	3.9326	0.0047	No
		41	70	0.271	0.045	3.9368	0.0059	No
		42	71	0.407	0.046	3.9540	0.0060	No
		43	72	0.429	0.056	3.9568	0.0072	No
		44	73	0.523	0.060	3.9686	0.0077	No
		45	74	0.505	0.075	3.9664	0.0096	No
		46	75	0.546	0.083	3.9715	0.0105	No
		47	76	0.58	0.11	3.9758	0.0139	No
		48	77	0.59	0.12	3.9771	0.0151	No
		49	78	0.58	0.12	3.9758	0.0152	No
30	Zn	32	62	−0.493	0.053	3.9031	0.0069	No
		33	63	−0.389	0.044	3.9164	0.0058	No
		34	64	−0.279	0.035	3.9305	0.0047	Yes
		35	65	−0.257	0.026	3.9333	0.0036	No
		36	66	−0.121	0.017	3.9505	0.0026	Yes
		37	67	−0.089	0.010	3.9546	0.0019	Yes
		38	**68**	**0**	–	**3.9658**	**0.0014**	Yes
		39	69	0.026	0.011	3.9691	0.0020	No
		40	70	0.142	0.016	3.9837	0.0024	Yes
		41	71	0.227	0.024	3.9943	0.0033	No
		42	72	0.292	0.031	4.0024	0.0041	No
		43	73	0.318	0.038	4.0057	0.0049	No
		44	74	0.375	0.045	4.0128	0.0058	No
		45	75	0.349	0.052	4.0096	0.0066	No
		46	76	0.421	0.058	4.0185	0.0073	No
		47	77	0.440	0.065	4.0209	0.0082	No
		48	78	0.474	0.071	4.0251	0.0089	No
		49	79	0.461	0.078	4.0235	0.0098	No
		50	80	0.465	0.085	4.0240	0.0107	No
31	Ga	32	63	−0.643	0.136	3.9308	0.0174	No
		33	64	−0.579	0.121	3.9390	0.0155	No
		34	65	−0.422	0.015	3.9589	0.0026	No
		35	66	−0.329	0.077	3.9706	0.0099	No
		36	67	−0.252	0.031	3.9803	0.0043	No
		37	68	−0.214	0.050	3.9850	0.0065	No
		38	69	−0.116	0.030	3.9973	0.0042	Yes
		39	70	−0.096	0.021	3.9998	0.0032	No
		40	**71**	**0**	–	**4.0118**	**0.0018**	Yes
		41	72	0.161	0.028	4.0318	0.0039	No
		42	73	0.243	0.043	4.0420	0.0056	No
		43	74	0.223	0.046	4.0395	0.0060	No
		44	75	0.285	0.059	4.0472	0.0075	No
		45	76	0.276	0.065	4.0461	0.0082	No
		46	77	0.308	0.075	4.0500	0.0094	No
		47	78	0.270	0.079	4.0453	0.0099	No
		48	79	0.290	0.088	4.0478	0.0110	No
		49	80	0.242	0.092	4.0418	0.0115	No
		50	81	0.242	0.099	4.0418	0.0124	No
		51	82	0.447	0.123	4.0671	0.0152	No
37	Rb	37	74	−0.045	0.143	4.1935	0.0172	No
		38	75	0.266	0.129	4.2305	0.0154	No
		39	76	0.298	0.116	4.2342	0.0139	Yes
		50	**87**	**0**	–	**4.1989**	**0.0021**	Yes
47	Ag	50	97	−1.29	0.22	4.4202	0.0250	No
		51	98	−1.01	0.18	4.4518	0.0204	No
		52	99	−0.91	0.14	4.4630	0.0159	No
		53	100	−0.83	0.12	4.4719	0.0137	No
		54	101	−0.70	0.12	4.4865	0.0136	Yes
		60	107	−0.15	0.05	4.5473	0.0060	Yes

(*continued on next page*)

Table 1 (*continued*)

Z	el.	N	A	$\delta\langle r^2\rangle$ (fm^2)	$\Delta\delta\langle r^2\rangle$ (fm^2)	r_c (fm)	Δr_c (fm)	In Ref. [1]
		62	**109**	**0**	–	**4.5638**	**0.0025**	Yes
48	Cd	52	100	−1.421	0.044	4.4519	0.0055	No
		53	101	−1.307	0.041	4.4647	0.0052	No
		54	102	−1.144	0.026	4.4829	0.0037	Yes
		55	103	−1.046	0.025	4.4938	0.0036	Yes
		56	104	−0.904	0.017	4.5096	0.0030	Yes
		57	105	−0.823	0.017	4.5185	0.0030	Yes
		58	106	−0.695	0.013	4.5327	0.0027	Yes
		59	107	−0.625	0.013	4.5404	0.0027	Yes
		60	108	−0.510	0.010	4.5530	0.0026	Yes
		61	109	−0.445	0.010	4.5602	0.0026	Yes
		62	110	−0.334	0.007	4.5723	0.0024	Yes
		63	111	−0.288	0.012	4.5773	0.0027	Yes
		64	112	−0.159	0.005	4.5914	0.0024	Yes
		65	113	−0.114	0.010	4.5963	0.0025	Yes
		66	**114**	**0**	–	**4.6087**	**0.0023**	Yes
		67	115	0.043	0.012	4.6134	0.0026	Yes
		68	116	0.134	0.009	4.6232	0.0025	Yes
		69	117	0.171	0.021	4.6272	0.0032	Yes
		70	118	0.243	0.023	4.6350	0.0034	Yes
		71	119	0.283	0.034	4.6393	0.0043	No
		72	120	0.342	0.038	4.6457	0.0047	Yes
		73	121	0.375	0.050	4.6492	0.0058	No
		74	122	0.431	0.055	4.6552	0.0063	No
		75	123	0.457	0.068	4.6580	0.0076	No
		76	124	0.510	0.073	4.6637	0.0081	No
		77	125	0.533	0.087	4.6662	0.0096	No
		78	126	0.585	0.091	4.6717	0.0100	No
		79	127	0.599	0.107	4.6732	0.0117	No
		80	128	0.660	0.108	4.6798	0.0118	No
		81	129	0.638	0.134	4.6774	0.0145	No
		82	130	0.705	0.133	4.6846	0.0144	No
50	Sn	58	108	−1.081	0.018	4.5579	0.0022	Yes
		60	110	−0.907	0.011	4.5770	0.0016	Yes
		62	112	−0.747	0.007	4.5944	0.0013	Yes
		64	114	−0.605	0.005	4.6098	0.0012	Yes
		66	116	−0.461	0.004	4.6254	0.0011	Yes
		68	118	−0.324	0.005	4.6402	0.0011	Yes
		70	120	−0.206	0.005	4.6529	0.0011	Yes
		72	122	−0.097	0.003	4.6646	0.0011	Yes
		74	124	0	–	4.6750	0.0010	Yes
		76	126	0.089	0.004	4.6845	0.0011	Yes
		78	128	0.165	0.010	4.6926	0.0015	Yes
		80	130	0.240	0.015	4.7006	0.0019	Yes
		82	132	0.307	0.021	4.7077	0.0024	Yes
		84	134	0.533	0.010	4.7317	0.0014	No
70	Yb	105	175	−0.0543	0.0002	5.3164	0.0062	Yes
		106	**176**	**0**	–	**5.3215**	**0.0062**	Yes
		107	177	0.0259	0.0001	5.3239	0.0062	No
80	Hg	97	177	−1.067	0.079	5.3474	0.0080	No
		98	178	−0.968	0.072	5.3567	0.0074	No
		99	179	−0.905	0.071	5.3626	0.0073	No
		100	180	−0.808	0.061	5.3716	0.0065	No
		101	181	−0.111	0.013	5.4361	0.0033	Yes
		102	182	−0.653	0.049	5.3860	0.0055	Yes
		103	183	−0.065	0.009	5.4403	0.0032	Yes
		104	184	−0.542	0.041	5.3963	0.0049	Yes
		105	185	−0.069	0.010	5.4400	0.0032	Yes
		118	**198**	**0**	–	**5.4463**	**0.0031**	Yes
81	Tl	98	179	−1.274	0.094	5.3583	0.0092	No
		99	180	−1.254	0.091	5.3602	0.0089	No
		100	181	−1.174	0.084	5.3676	0.0083	No
		102	183	−1.033	0.074	5.3786	0.0074	No
		104	185	−0.938	0.078	5.3896	0.0077	No
		109	190	−0.7063	0.0490	5.4110	0.0052	Yes
		110	191	−0.6544	0.0460	5.4158	0.0050	Yes
		111	192	−0.6296	0.0440	5.4181	0.0048	Yes
		112	193	−0.5716	0.0400	5.4235	0.0045	Yes
		113	194	−0.5551	0.0063	5.4250	0.0027	Yes
		114	195	−0.4820	0.0347	5.4317	0.0041	Yes
		115	196	−0.4795	0.0340	5.4319	0.0041	Yes

(*continued on next page*)

Table 1 (*continued*)

Z	el.	N	A	$\delta\langle r^2\rangle$ (fm^2)	$\Delta\delta\langle r^2\rangle$ (fm^2)	r_c (fm)	Δr_c (fm)	In Ref. [1]
		116	197	−0.4119	0.0299	5.4382	0.0038	Yes
		117	198	−0.4035	0.0289	5.4389	0.0037	Yes
		118	199	−0.3116	0.0231	5.4474	0.0034	Yes
		119	200	−0.2979	0.0222	5.4486	0.0033	Yes
		120	201	−0.2077	0.0150	5.4569	0.0030	Yes
		121	202	−0.1834	0.0148	5.4591	0.0029	Yes
		122	203	−0.1032	0.0070	5.4665	0.0027	Yes
		123	204	−0.0635	0.0081	5.4701	0.0027	Yes
		124	**205**	**0**	–	**5.4759**	**0.0026**	Yes
		126	207	0.1048	0.0070	5.4855	0.0027	Yes
		127	208	0.183	0.019	5.4926	0.0031	Yes
83	Bi	**126**	**209**	**0**	–	**5.5211**	**0.0026**	Yes
		128	211	0.221	0.017	5.5411	0.0031	No
		130	213	0.422	0.029	5.5592	0.0038	Yes
84	Po	109	193	−0.576	0.013	5.5185	0.0178	No
		111	195	−0.604	0.013	5.5159	0.0178	No
		113	197	−0.657	0.013	5.5111	0.0178	No
		115	199	−0.644	0.013	5.5123	0.0178	No
		117	201	−0.510	0.013	5.5244	0.0178	No
		119	203	−0.425	0.013	5.5321	0.0178	No
		125	209	−0.0813	0.0100	5.5631	0.0176	Yes
		125	**210**	**0**	–	**5.5704**	**0.0176**	Yes
		127	211	0.104	0.010	5.5797	0.0176	No
		133	217	0.821	0.018	5.6436	0.0174	No
		134	218	0.948	0.013	5.6549	0.0174	Yes
87	Fr	115	202	−1.596	0.018	5.5367	0.0182	No
		116	203	−1.530	0.018	5.5427	0.0182	No
		117	204	−1.571	0.018	5.5390	0.0183	No
		118	205	−1.475	0.017	5.5476	0.0182	No
		119	206	−1.465	0.017	5.5485	0.0182	No
		134	**221**	**0**	–	**5.6790**	**0.0177**	Yes
88	Ra	**126**	**214**	**0**	–	**5.6079**	**0.0177**	Yes
		134	222	1.0449	0.0524	5.7003	0.0180	Yes
		125	223	1.1708	0.0587	5.7113	0.0181	Yes
		136	224	1.2680	0.0636	5.7198	0.0182	Yes
		137	225	1.4041	0.0704	5.7317	0.0184	Yes
		138	226	1.4858	0.0745	5.7388	0.0185	Yes
		139	227	1.5871	0.0796	5.7477	0.0186	Yes
		140	228	1.6980	0.0852	5.7573	0.0188	Yes
		141	229	1.8102	0.0908	5.7670	0.0189	Yes
		142	230	1.9435	0.0975	5.7786	0.0191	Yes
		143	231	2.0177	0.1012	5.7850	0.0193	No
		144	232	2.1589	0.1083	5.7972	0.0195	Yes
		145	233	2.225	0.115	5.8029	0.0198	No